ICMIEE22-087

Design and Simulation of Wireless Power Transmission System for E-Bike.

Muhammad Faiz Ahmed[1,*], *Murad Hossain*[2], *MD. Helal-An-Nahiyan*[3]
[1] Department of Mechanical Engineering, Khulna University of Engineering & Technology, Khulna-9203, BANGLADESH
[2] Department of Electrical & Electronics Engineering, Khulna University of Engineering & Technology, Khulna-9203, BANGLADESH
[3] Department of Mechanical Engineering, Khulna University of Engineering & Technology, Khulna-9203, BANGLADESH

ABSTRACT
The use of wireless power transfer (WPT) technologies has become very popular in recent times all around the world. Contactless inductive power transfer (IPT) allows electrical energy to be transferred to fixed or moving consumers without the use of contacts, cables, or slip rings. WPT applications are fast developing not just in small power devices such as wireless charging for mobiles and electric toothbrushes, but also in the field of electric vehicles and other niche fields as it is proving more convenient and flexible system for consumers. In this research, A stationary wireless power transmission system for electric vehicle charging applications is studied and analyzed. A simulation model of spiral-shaped magnetic coupler with a ferrite core is developed to transfer 431W power over a 15cm air gap for charging a DC160-12 battery which is commonly used in electric autos in Bangladesh. This simulated model can help us to build prototypes of wireless power transmission charging systems for electric vehicles in the near future. The methodology for developing the system is divided into two main sections: one is to develop the magnetic structure through designing and performing simulation to determine the parameters and the other one is to design and simulate the electronic circuit. The magnetic structure has been developed and simulated in the 'Ansys Electronics Desktop 2021 R1' and 'Matlab R2020a' platform has been used for electronic circuits. A series-series resonant topology is adopted as the wireless power transfer DC-DC stage due to the advantages of circuit simplicity, easy analysis, and control. The proposed model can supply 20.84A constant DC current which can fully charge the battery within 7.6 hours and operates at 20 kHz resonant with 72 % power transfer efficiency in a 15cm air gap. The model also shows good resilience in horizontal miss-alignment.

Keywords: WPT, Electric vehicle (EV), Inductance, Transmitter coil, Receiver coil.

1. Introduction

In recent times, Wireless power transmission (WPT) systems getting more and more attention all over the world due to their numerous advantages over wired connections. The most common uses of the WPT system are induction cooking and mobile charging. But recently it has gained the attention of a lot of researchers due to its promising future in electric vehicle charging applications [1-3] and biomedical implant applications [4].

Even though electricity is magnetically carried from the source to the load via larger air gaps, inductive wireless power transfer (IPT) systems use mutual coupling between two coils, similar to what is done in traditional transformers, to transmit power. The effectiveness of power transfer in the system is significantly influenced by the design of the employed transformer. [5-8].

Tesla proposed the idea of wireless power transfer (WPT) near the end of the nineteenth century. He developed a wireless lighting bulb that transmits electrical energy. He used two plates of metal that were close to one another. Bypassing high-frequency Alternate Current (AC) potentials between these two metal plates, the bulb was turned on. But, numerous issues developed as a result of implementing WPT technology. One significant problem is that the tiny power density and low transfer efficiency become more pronounced as distances increase. The result is a severe decline in WPT technology performance. As a result, "strong linked" coils are currently utilized to wirelessly charge at distances larger than 2 meters because of advancements in WPT technology. The two fundamental WPT Technologies are inductive power transfer (IPT) and capacitive power transfer (CPT). The CPT, however, is only suitable for low-power applications with extremely small air gaps of 10-4 to 10-3 m., whereas IWPT is the most extensively used WPT technology since it can manage vast air gaps of several meters and has a significantly higher output power than CPT [9].

In the 1900s electric vehicles (EVs) were initially well-received with 38% of automobile sales but it was quickly phased out due to economical and technical reasons. Beginning of the 1930s, gasoline, and the diesel engine was ruling the automobile industries, and still, most automobile engines run on fossil fuels. As a result, cities are suffocating under the weight of pollution and also the storage of fossil fuels is running out. Therefore, scientists are looking for alternatives and again turning towards electrically powered automobiles. In two of the last decades, solid-state power electronics had been improved for brushless electric motors, and higher-capacity lithium batteries have all been available. A flood of new electric car designs has reignited interest

* Corresponding author. Tel.: +88-01620711545
E-mail addresses: faiz.140509@gmail.com

in the industry, and current estimates indicate that the use of this technology will rise. Despite their superior performance in terms of energy density and life cycle, modern batteries are still unable to match the higher autonomy and lower cost of contemporary fuel-based cars. Battery recycling and city planning for the enormous number of people required for charging stations with plugs may also have an impact on the widespread adoption of EVs. Other issues may also have an impact on this. The dynamic and stationary wireless power transfer technique has drawn a lot of interest as a result of these worries. [10].

A secondary coil (Rx) is attached to the load in a standard loosely coupled IWPT system while connected to a high-frequency (HF) AC source is the transmitter coil (Tx). A voltage is created across the Tx when HF current flows through it and is coupled with the Rx, creating an electromagnetic field. A power converter attached to Tx transforms utility electricity (from the AC grid or a DC battery) into HF AC, and between Rx and the electrical load, a rectifier circuit is connected. The maximum energy may be transferred when Rx resonates at the same resonance frequency as the HF source. A WPT scheme that uses a fixed WPT Rx during power transmission is referred to as stationary WPT. A novel development of stationary WPT called dynamic WPT attempts to wirelessly power the moving receiver (Rx). Medicinal applications [11], electric vehicles [12], robotics [13], and manufacturing [14] could all benefit from using dynamic WPT. However, the actual aim of this research is the analysis of stationary charging of electric vehicles (EVs), as dynamic WPT is yet not feasible from Bangladesh's perspective.

2. Fundamental Analysis

2.1 Fundamental structure

As illustrated in Fig. 1, an IWPT transformer can be modeled using the mutual inductance principle. Here, L_1 is the primary winding self-inductance, L_2 is the secondary winding self-inductance, R1 is the primary winding resistance, and M is the mutual inductance.

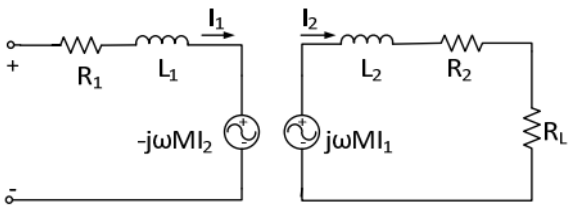

Fig.1 Basic IWPT circuit.

Considering sinusoidal voltages and currents, $j\omega MI_1$ represents the voltage that the main side's current will cause in the secondary side. In the same way, where is the operational frequency, the voltage reflected in the primary side due to the current of the secondary side is equal to $-j\omega MI_2$. R_L is a symbol for a resistive load.

2.2 Equivalent Circuit Theory

The basic IWPT circuit can be expressed by the following equivalent circuit.

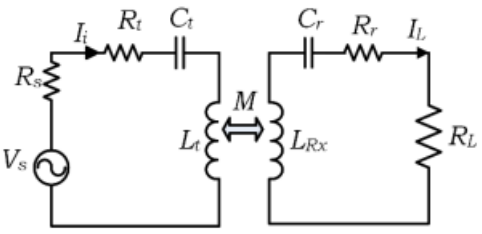

Fig.2: Equivalent circuit of basic IWPT circuit.

Kirchhoff's voltage law can be used in the equivalent circuit to create the following formulas.

$$\begin{bmatrix} Z_t + R_s & j\omega M \\ j\omega M & Z_r + R_L \end{bmatrix} \begin{bmatrix} I_i \\ I_L \end{bmatrix} = \begin{bmatrix} V_s \\ 0 \end{bmatrix}$$

$$Z_{t,r} = R_{t,r} + j\omega L_{t,r} + \frac{1}{j\omega C_{t,r}} \text{ and } M = k\sqrt{L_t L_r}$$

Where Vs is the RMS voltage of the HF source with a fundamental frequency and Zt and Zr are the impedances of the transmitter and receiver resonators, respectively Lt,r, Ct,r, and Rt,r, respectively, stand for the coils' inductance, capacitance, and resistance. Both the distributed capacitance of the coil and the externally applied lumped capacitance are referred to as capacitance. Mutual inductance (M) between the transmitter and receiver can be expressed using coupling coefficient (k) and coil inductances. The following formulas can be used to calculate output power at the load and power transfer efficiency (PTE):

$$P_{\text{out}} = |I_L|^2 R_L$$

$$PTE = \frac{|I_L|^2 R_L}{|I_i|^2 (R_t) + |I_L|^2 (R_L + R_r)}$$

$$\text{where } I_i = \frac{(R_L + Z_r) V_s}{(Z_t + R_S)(R_L + Z_r) + (\omega M)^2}$$

$$\text{and } I_L = \frac{(j\omega M) V_s}{(Z_t + R_S)(R_L + Z_r) + (\omega M)^2}$$

The reactive impedance of the coil is zero at resonance frequency conditions. The transmitter and receiver coils' resonant frequencies become,

$$X_{t,r} = j\omega_{t,r} L_{t,r} + \frac{1}{j\omega_{t,r} C_{t,r}} = 0 \rightarrow \omega_{t,r} = \frac{1}{\sqrt{L_{t,r} C_{t,r}}}$$

The equivalent circuit approach can be used to calculate element parameters including currents and voltages across coils, as well as compensation capacitors. As a

result, while building a high-power WPT system, applying comparable circuit-based analysis to determine component ratings is crucial.

2.3 Basic Topologies

SS, SP, PS, and PP are the four fundamental topologies. The letters S and P stand for series and parallel compensation of primary or secondary circuits, with the first letter denoting the primary circuit and the second letter denoting the secondary circuit, respectively. Parallel compensation involves connecting a compensation capacitor in parallel with the primary or secondary leakage inductance, while series compensation means connecting a compensation capacitor in series with it. The SS topology is the most fundamental and is frequently employed because it is simple to analyze and manage.

2.4 Operating Frequency

The frequency of operating a WPT system must be determined while taking into account a range of technical and regulatory constraints that differ by country. When it comes to a WPT system's maximum potential efficiency, the highest quality factor is preferable. Increase coil inductance, raise operating frequency, or decrease coil resistance to increase the quality factor. However, when the frequency grows, AC resistance rises owing to skin effect losses. A coil's inductance, on the other hand, is governed by its shape and essentially unaffected by the operating frequency. As a result, a perfect frequency is there for a certain design type to achieve the highest potential quality factor. The optimal frequency for most designs is in the MHz range. Designing a high-power WPT system in the MHz range with today's semiconductor capabilities, however, remains tough. As a result, device ratings set the top limit for operational frequency. Frequencies ranging from 10 kHz to 150 kHz have been effectively used for high-power applications such as electric vehicles, while for applications that require lower power for instance biomedical applications operating frequencies as high as 20MHz have been successfully implemented. A frequency of 20kHz is taken as the operating frequency for this investigation.

3. Model

3.1 Coil design

The simulation software used to perform the modeling task is 'Ansys Electronics Desktop 2021 R1' and 'Matlab R2020a'.

Table 1 Dimensions of the spiral coil.

Parameters	Dimension
Outer dia, D	250 mm
Inner dia, d	100 mm
Number of turns	20
Pitch	3 mm
Conductor thickness	1.5 mm
Ferrite bar	95mm×20mm×5mm
Number of ferrite bar	9

The Tx and Rx coil, both have the same geometry, and the coil conductor material is copper.

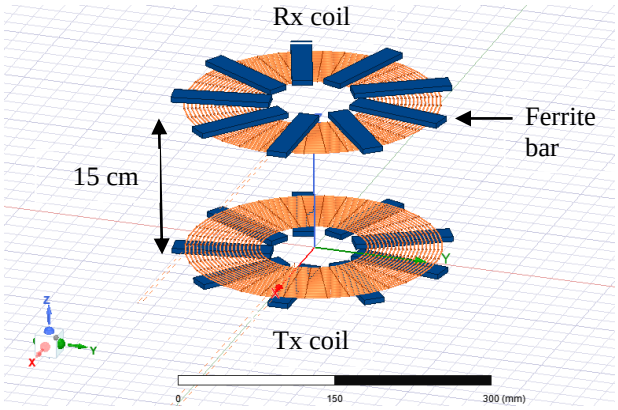

Fig.1 Spiral-shaped Tx and Rx coil.

3.2 Circuit Design

The power transmission circuit is designed in Matlab Simulink R2020a. It mainly comprises three parts: 1. High-frequency inverter at primary side, 2. Resonant capacitors and couplers, 3. Full bridge rectifier and load at the secondary side. In the design, four IGBT/Diode is used to build the inverter and four Diode is used to build the rectifier.

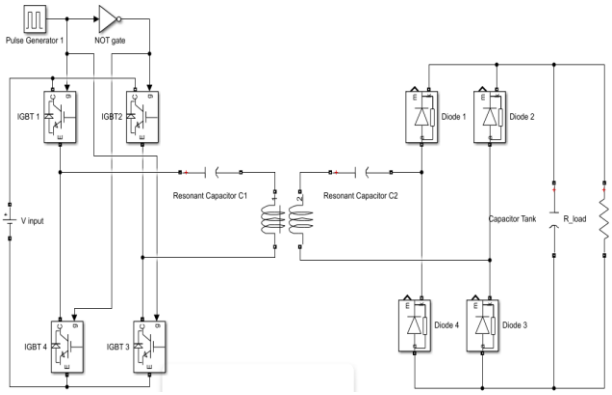

Fig.4 Diagram of the power transmission circuit.

Table 2 Input parameters and values of power transmission circuit.

Parameters	Value
DC input voltage, V_{in}	40 v
Primary resonant capacitance, C_1	520 nF
Secondary resonant capacitance, C_2	520 nF
External resistance or load resistance, R	1Ω
Primary self-inductance, L_t	121.7 µH
Secondary self-inductance, L_r	121.7 µH
Mutual inductance, M	11.8 µH
Coupling coefficient, k	0.1

4. Result and Discussion

4.1 Coil Simulation

The parameters like mutual induction, coupling coefficient, and self-inductances are measured for varying transfer distance and horizontal misalignment between primary and secondary coils during coil simulation. The following data and graph are achieved from the simulation.

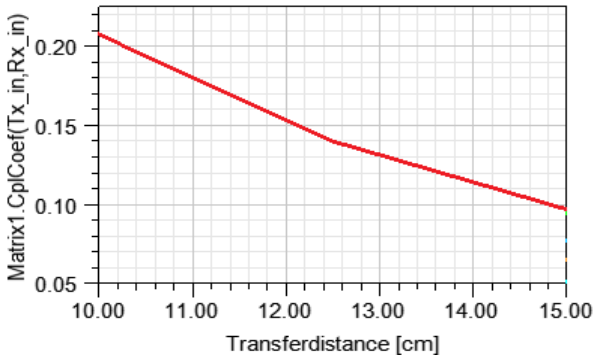

Fig.5 Coupling coefficient vs distance graph.

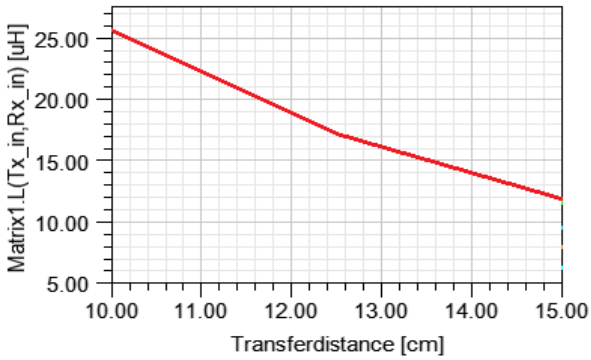

Fig. 6 Mutual inductance vs distance graph

Above two figures, fig. 4.1 and 4.2 illustrates the coupling co-efficient and mutual inductance vs distance curve. The graph shows that the coupling coefficient is decreasing with the distance which is as predicted. It is quite obvious that the coupling coefficient will decrease with the distance as the leakage inductance increases and the magnetic field becomes weaker. From the fundamental analysis we got the expression, $M = k\sqrt{L_p L_S}$, so the mutual inductance is directly proportional to the coupling coefficient if the self-inductance remains constant. The mutual inductance vs distance graph shows the same property as the coupling coefficient graph, the mutual inductance is decreasing with the distance as the self-inductance remains nearly constant.

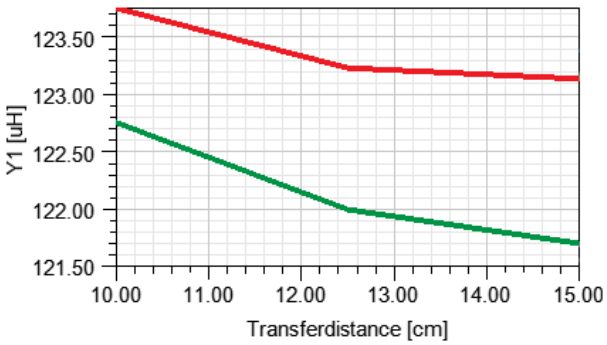

Fig. 7 Self-inductances of Tx and Rx coil vs transfer distance.

In fig.7, the self-inductance of the Tx and Rx coil has been plotted against the transfer distance. Here the red line denotes Rx coil self-inductance and the green line denotes Tx coil. Because both coils have the same geometry and self-inductance should not be affected by transfer distance, the two lines should intersect and be a straight line. However, this is not the case; the Rx coil inductance is somewhat higher than the Tx coil inductance, and the self-inductance decreases significantly with distance. While some experts speculate that it could be due to the secondary side's reflected impedance and vice versa when measuring the coils' self-inductance, no clear explanation has been uncovered. However, the difference is not significant (below 2 percent).

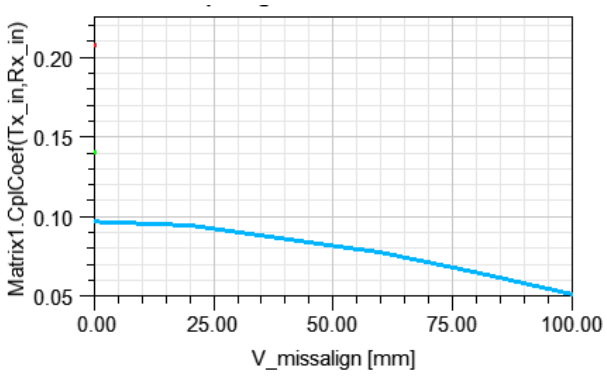

Fig. 8 Coupling coefficient vs Horizontal miss-alignment graph at 15 cm transfer distance.

Fig.8 shows the change of coupling coefficient with the horizontal miss-alignment at a 15 cm transfer distance. The coupling coefficient decreases with the increasing miss-alignment. This curve has the same characteristic as the coupling coefficient vs transfer distance curve as the reason behind decreasing the coupling coefficient is the same for both cases.

Table 3 Data of k, M and L with transfer distance.

Transfer Distance	k	M (µH)	L_t (µH)	L_r (µH)
10 cm	0.2	25.53	122.7	123.74
12.5 cm	0.14	17.13	121.9	123.22
15 cm	0.1	11.8	121.7	123.13

Table 4 Data of k, M, and L with horizontal miss-alignment

Horizontal miss-alignment(mm)	k	M (µH)	L_t (µH)	L_r (µH)
20	0.94	11.56	121.7	123.125
60	0.77	9.49	121.63	123.3
100	0.05	6.27	121.55	123.16

4.2 Power Transmission Circuit

Power transfer circuit simulation is done in the Matlab Simulink R2020a and through the simulation, the values of current, voltage, and efficiency had been obtained in different phases of the circuit after passing the inverter, in the secondary side, and after rectifying. Here all the coil simulation values of 15cm transfer distance are taken as input as we want to transfer the power at a 15cm air gap. The circuit is built such so that it can charge the DC160-12 battery efficiently with high efficiency. So, a 40v DC source is taken as the input voltage, and the measured input current is I_{in}=15.01A. The following data and graphs are obtained during the whole circuit simulation.

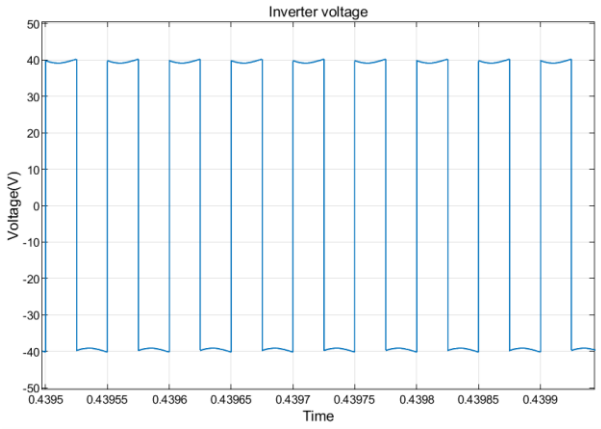

Fig. 9 Waveform of voltage after passing the inverter.

The peak voltage of the square can be measured from the above fig.9 which is 40V.
The RMS value of this square wave voltage after passing the inverter is V_{rms}= 39.48V.
Metal oxide semiconductor field-effect transistor (MOSFET, IGBT) devices are frequently employed to generate square waves due to their rapid on-off electronic switching characteristic, as opposed to BJT transistors, which produce signals that resemble sine waves rather than square waves.

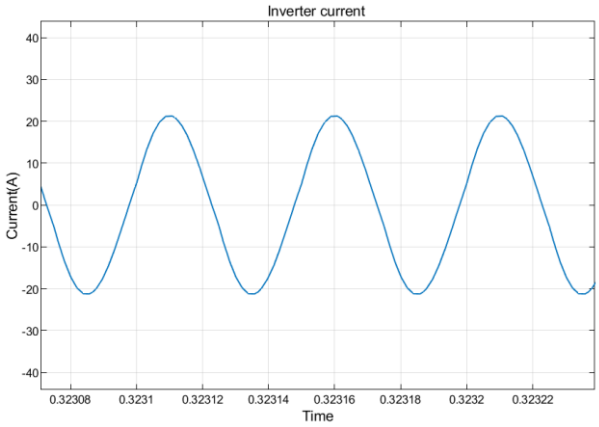

Fig. 10 Waveform of current after passing the inverter.

From the sine plot of inverter current in fig.10, the peak value of current after passing the inverter can be measured which is 21.2A. The RMS value of this sine wave current after passing the inverter, I_{rms}= 15A.
So, the efficiency of the inverter = $(V_{rms}I_{rms})_{inverter}$ / $(V_{in}I_{in})$ = 0.986 = 98.6%
There are minor losses in the IGBT diode.

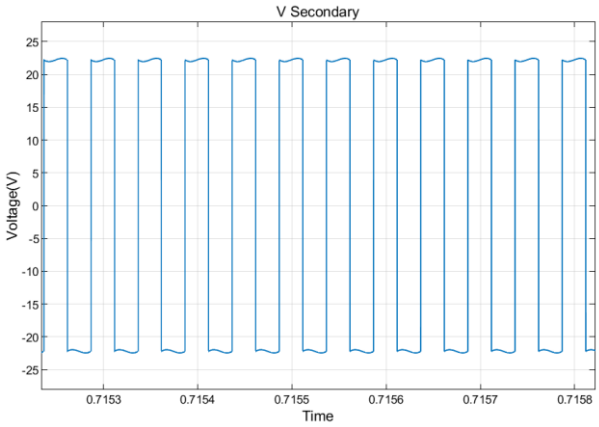

Fig. 11 Waveform of AC voltage on the secondary side.

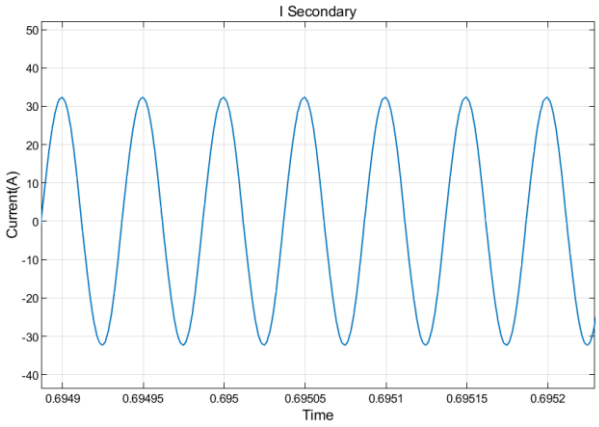

Fig. 12 Waveform of AC current on the secondary side.

In Fig.11 and Fig.12 the time-varying current and voltage graph against time has been plotted. From the plots, the peak value of voltage and current can be measured. The peak value of AC voltage on the secondary side is 22.25V and the peak value of AC current is 32.24. The RMS values of AC voltage and current are also measured by the RMS (mask) block in the Simulink.

The RMS values of voltage and current on the secondary side are 22.15V and 22.97A, respectively.

So, The coil efficiency = $(V_{rms}I_{rms})/(V_{rms}I_{rms})_{inverter}$ = 0.86 = 86%

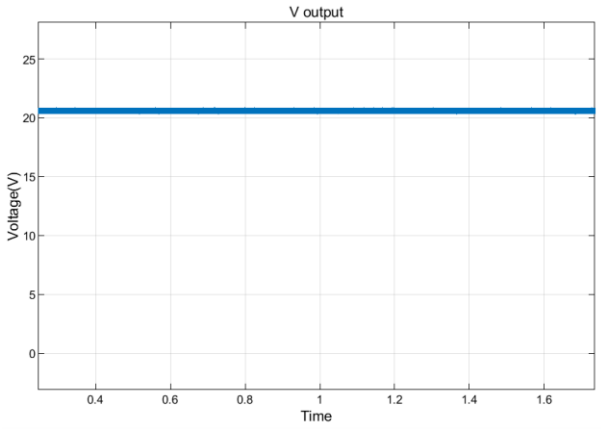

Fig. 13 Final DC output voltage after rectifying.

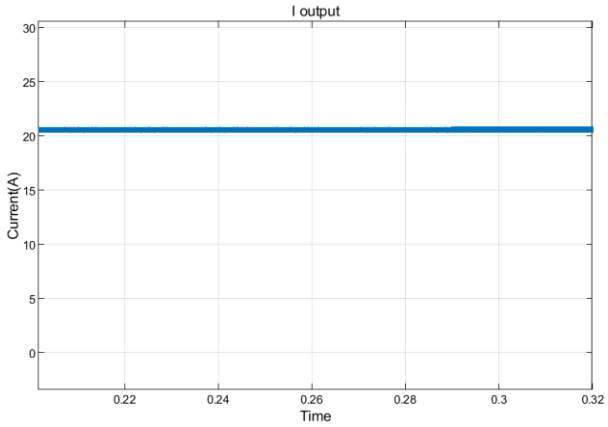

Fig. 14 Final output DC current after rectifying.

In fig.13 and fig.14 ., the straight blue line shows the DC output voltage and DC output current after rectifying the AC and the values are 20.71V and 20.84A respectively.

The total output power of the whole system = $V_{out} \times I_{out}$ = 431.6 W

The efficiency of rectifier = $(V_{out}I_{out})/(V_{rms}I_{rms})_{secondary}$ = 85 %

Table 5 Value of voltage, current, and efficiency of different sections of the circuit.

Horizontal miss-alignment (mm)	Overall Efficiency
20 mm	69.8 %
60 mm	62.6 %
100 mm	53.5 %

Table 6 Table for Overall efficiency with increasing horizontal miss-alignment.

Section	Voltage(V)	Current(A)	Efficiency
Inverter (RMS) value	39.48	15	98.6 %
Secondary (RMS) value	22.15	22.97	86 %
Rectifier (DC) value	20.71	20.84	85 %
The overall efficiency			72 %

Using the coil simulation data, efficiency has been measured for increasing horizontal miss-alignment.

From the data of table 6, it can be observed that at first frequency was decreasing slowly with the miss alignment. However, as the horizontal misalignment increases, the efficiency decreases. For example, the efficiency has declined by 7.2% for 20mm to 60mm and 9.1% for 60mm to 100mm horizontal miss-alignment, but both have the same alignment gap. The efficiency will drop more quickly for further miss-alignment and at some point, it will decrease drastically. The same characteristics can be observed in the curve of coupling coefficient vs horizontal miss-alignment curve. Its because the coupling coefficient has a direct effect on the transfer power efficiency.

5. Conclusion

In this research, the magnetic structure of the WPT spiral coil and resonant electronic circuit of the WPT system has been analyzed and implemented for EV charging applications. System configuration and design factors were examined and talked about. A WPT coil of spiral structure has been optimized and simulated in Ansys Maxwell 3D. A simulative model of 431W is designed and simulated in the Matlab Simulink to charge a DC160-12 battery. The system can supply 20.84A constant DC current which is capable of fully charging the battery within 7.6 hours, whereas the conventional wired charging system takes 12 hours to fully recharge the battery. The WPT system operates at 20kHz resonant frequency and power transfer efficiency is 72% with a 15 cm air gap at 431W rated power and input condition 40V. This wireless power transmission system is developed for stationary charging systems of electric vehicles. The transmitter coil can be mounted upon or beneath the ground of the parking lot and the receiver coil will be mounted under the vehicle chassis. With some sophisticated adjustments, this method can also be used for dynamic wireless charging of electric automobiles.

References

[1] S. Li and C. C. Mi, "Wireless Power Transfer for Electric Vehicle Applications," *Emerging and Selected Topics in Power Electronics, IEEE Journal of*, vol. 3, pp.4-17, 2015.

[2] T. Imura, H. Okabe, and Y. Hori, "Basic experimental study on helical antennas of wireless power transfer for Electric Vehicles by using magnetic resonant couplings," in *Vehicle Power and Propulsion Conference, 2009. VPPC '09. IEEE*, 2009, pp.936-940.

[3] U. K. Madawala and D. J. Thrimawithana, "A Bidirectional Inductive Power Interface for Electric Vehicles in V2G Systems," *Industrial Electronics, IEEE Transactions on*, vol. 58, pp. 4789-4796, 2011.

[4] R. F. Xue, K. W. Cheng, and M. Je, "High-Efficiency Wireless Power Transfer for Biomedical Implants by Optimal Resonant Load Transformation," *Circuits and Systems I: Regular Papers, IEEE Transactions on*, vol. PP, pp. 1-1, 2012.

[5] Xiu Zhang, S. L. Ho, W. N. Fu, "Quantitative Design and Analysis of Relay Resonators in Wireless Power Transfer System," *Magnetics, IEEE Transactionson*, vol.48,no.11, pp. 4026, 4029, Nov.212.

[6] S. Chopra, V. Prasanth, B. E. Mansouri, P. Bauer, "A contactless power transfer — Supercapacitor based system for EV application," *IECON 2012 - 38th Annual Conference on IEEE Industrial Electronics Society* , vol., no., pp.2860,2865, 25-28Oct.2012.

[7] A.Neves, D.M. Sousa, A. Roque, J. M. Terras, "Analysis of an inductive charging system for a commercial electric vehicle," *Power Electronics and Applications (EPE 2011), Proceedings of the 2011-14th European Conference on*, vol., no., pp.1,10, Aug. 30 2011-Sept. 1 2011.

[8] H. H. Wu, A. Gilchrist, K. D. Sealy, D. Bronson, "A High Efficiency 5 kW Inductive Charger for EVs Using Dual Side Control," *Industrial Informatics, IEEE Transactions on*, vol.8, no.3, pp.585,595, Aug. 2012.

[9] N. Iqteit, K. Yahya, and S. A. Khan, "Wireless Power Charging in Electrical Vehicles," *Wirel. Power Transf. – Recent Dev. Appl. New Perspect.*, Feb. 2021, doi: 10.5772/INTECHOPEN.96115.

[10] L. A. L. Cardoso, M. C. Martinez, A. A. N. Meléndez, and J. L. Afonso, "Dynamic inductive power transfer lane design for E-Bikes," *IEEE Conf. Intell. Transp. Syst. Proceedings, ITSC*, pp. 2307–2312, Dec. 2016, doi: 10.1109/ITSC.2016.7795928.

[11] N. Kyungmin, J. Heedon, M. Hyunggun, and F. Bien, "Tracking Optimal Efficiency of Magnetic Resonance Wireless Power Transfer System for Biomedical Capsule Endoscopy," *IEEE Transactions on Microwave Theory and Techniques*, vol. 63, no. 1, pp. 295-304, 2015.

[12] T. Ando, H. Omori, N. Kimura, and T. Morizane, "A Novel Type of Dynamic Wireless Power Transferred Scooter System with EDLC Storage Unit," *Asia-Pacific Power Energy Eng. Conf. APPEEC*, vol. 2019-Decem, Dec. 2019, doi: 10.1109/APPEEC45492.2019.8994349.

[13] J. P. C. Smeets, T. T. Overboom, J. W. Jansen, and E. A. Lomonova, "Comparison of PositionIndependent Contactless Energy Transfer Systems," *IEEE Transactions on Power Electronics*, vol. 28, no. 4, pp. 2059-2067, 2013.

[14] J. P. C. Smeets, T. T. Overboom, J. W. Jansen, and E. A. Lomonova, "Modeling Framework for Contactless Energy Transfer Systems for Linear Actuators," *IEEE Transactions on Industrial Electronics*, vol. 60, no. 1, pp. 391-399, 2013.

NOMENCLATURE

Tx	: Transmitter side
Rx	: Receiver side
L	: Self inductance, µH
k	: Coupling co-efficient
M	: Mutual inductance, µH
L_s	: Primary coil self inductance, µH
L_p	: Secondary coil self inductance, µH